PHYSICAL REVIEW B VOLUME 40, NUMBER 6 15 AUGUST 1989-II

Disruption, atom distributions, and energy levels for Ge/GaAs(110), Ge/InP(110), and Ge/InSb(110) heterojunctions

C. M. Aldao, I. M. Vitomirov, F. Xu, and J. H. Weaver
Department of Chemical Engineering and Materials Science, University of Minnesota, Minneapolis, Minnesota 55455
(Received 15 July 1988; revised manuscript received 23 February 1989)

We report a detailed room-temperature synchrotron-radiation photoemission study of Ge overlayer growth on *n*-type GaAs(110), InP(110), and InSb(110) in order to correlate changes in bonding configurations and atom distribution with the movement of the Fermi level in the substrate band gap and the evolution of the electronic properties of the Ge overlayer. For Ge/GaAs(110), the interface is abrupt, but substrate core-level line-shape analysis indicates changes in the boundary layer and unique interface bonding configurations. Ge adatoms induce substrate disruption for InP(110) and InSb(110), and there are coverage-dependent morphology changes as atoms dissociated from the substrate redistribute themselves in the thickening Ge overlayer. In atoms segregate to the Ge surface but exhibit no tendency to form clusters; P atoms remain near the buried Ge/InP interface; and Sb atoms are expelled to the overlayer surface. The deposition of Ge on GaAs and InP causes the Fermi level to move toward midgap at low coverage, but then move back toward the conduction band. The reversal in direction correlates well with changes in substrate core-level line shapes. Low-temperature studies of Ge/*n*-type GaAs did not show this reversal, but the final position of E_F in the gap was the same. The fully developed valence-band discontinuities were 0.73, 1.03, and 0.12 eV for amorphous Ge/GaAs(110), Ge/InP(110), and Ge/InSb(110) heterojunctions, respectively.

INTRODUCTION

Interfaces have come under increased scrutiny, in part because they exhibit unique structural, electronic, and chemical properties. For semiconductor heterojunctions, the fact that the two semiconductors have different energy gaps results in valence and conduction-band discontinuities. In turn, these offsets play a crucial role in the electrical properties of the heterojunction,[1,2] and they can be used in the design of solid-state electronic devices. Despite significant advances of the past few years, many fundamental questions remain.[3–6]

Most theoretical treatments of heterojunction band lineups have assumed abrupt, lattice-matched interfaces.[7] Likewise, most assume that there is an absolute energy associated with each semiconductor so that the band offsets reflect differences in those energies. Experimentally, however, it has been observed that the electrical properties can be related to the chemical and geometric structure at the interface and can be dictated by deviations from perfection.[5,8,9] In particular, band offsets can depend on such variables as substrate orientation, overlayer crystallinity, the order of deposition, and interdiffusion or reactivity. In such cases, there is no unique value for the lineup and experiments must therefore provide better insight into structure-property correlations for heterojunctions.

In this paper, we present synchrotron-radiation photoemission studies of room-temperature Ge overlayer growth on *n*-type GaAs(110), InP(110), and InSb(110). These results show that adatoms of Ge induce changes which can be readily observed by high-resolution core-level photoemission. For InP(110) and InSb(110), we show that there is substrate disruption and the release of In, P, and Sb. The coverage-dependent atom distributions for these released atoms reflect segregation of In and Sb and the retention of P near the buried interface. In no case is there evidence for cluster formation of the released atoms. With these results we can correlate the electronic configuration of the interface reflected in the coverage-dependent position of the Fermi level in the band gap. In particular, we observe an interesting movement of E_F toward midgap for low coverage but then a reversal which is associated with changes in the atom profiles (for InP) and interface bonding configurations (for GaAs). At high coverage, the valence-band offset is 0.73 eV for Ge/GaAs, 1.03 eV for Ge/InP, and 0.12 eV for Ge/InSb.

EXPERIMENT

Photoemission experiments were done at the Aladdin electron storage ring at the Wisconsin Synchrotron Radiation Center using the Mark V and Mark II Grasshopper monochromators and beamlines. Electrons were energy analyzed with a commercial double-pass cylindrical mirror analyzer. The total experimental resolution (monochromator plus analyzer) was $\sim$200 meV for the In 4*d*, Ga 3*d*, As 3*d*, and Sb 4*d* core levels, $\sim$400 meV for the P 2*p* core levels, and $\sim$300 meV for the valence bands. With synchrotron radiation, it was possible to adjust the kinetic energy of the photoelectrons so as to vary the surface sensitivity of the measurements.[10] In these studies, we used two different photon energies to investigate the evolving interfaces with two different probe depths. Experimental escape depths were calculated to be $\sim$4 Å for

 ©1989 The American Physical Society

the surface-sensitive measurements and 7–12 Å for those with higher bulk sensitivity.

Posts of GaAs, InP, and InSb were cleaved *in situ*. The quality of each cleave was judged visually and by inspection of the core levels and valence-band spectra. InP was Sn doped at 4×10^{17} cm^{-3}, GaAs was Si doped at 2×10^{18} cm^{-3}, and InSb was Te doped at 4×10^{15} cm^{-3}. Ge was evaporated from resistively heated tungsten boats at pressures $\leq 4\times10^{10}$ Torr in a system with an operating pressure of 8×10^{-11} Torr. Evaporation rates were $\sim$1 Å/min, and the source to sample distance was $\sim$35 cm. Overlayer depositions were monitored by an oscillating quartz crystal. The amount of deposited Ge is expressed in units of angstroms. Conversion from angstroms to monolayers yields 0.5 ML/Å for GaAs(110), 0.54 ML/Å for InP(110), and 0.65 ML/Å for InSb(110) with the assumption that the overlayer grows in registry with the substrate.

Line-shape analysis of the various core-level spectra was done with an IBM PC/RT computer using a nonlinear least-squares minimization procedure.[11] Spectral line shapes were represented by Voigt functions (the convolution of Lorentzian and Gaussian functions) to describe the natural core-level shape and to account for effects due to phonon broadening and instrumental response. As many as three spin-orbit doublets were allowed during the fitting procedures. As we will see, such detailed line-shape analysis is essential to reveal chemical changes during interface evolution and to correlate the band offset to those changes.

To determine the valence-band discontinuity, we measured the energy difference between the valence-band maximum for the cleaved surface and for the overlayer at each stage during growth.[12] These valence-band maxima (VBM) were obtained by extrapolating the leading edge of the energy distribution curves (EDC's) to the energy axis, an approximation which is reasonable if the spin-orbit splitting of the semiconductor states near the valence-band maximum is small. It is a less precise method than the method described by Waldrop *et al.*,[8] but it gave a precision of ±0.05 eV. (Although the linear extrapolation cannot satisfactorily determine the exact position of the VBM, their differences can be successfully measured, as discussed by List and Spicer.[13]) Simultaneously, we corrected for changes in band bending, as obtained directly from the bulk component of the substrate core-level emission.

RESULTS AND DISCUSSION

Ge/*n*-type GaAs(110)

The Ge/GaAs(110) system is probably the most studied heterojunction.[14] It has attracted much attention because of the nearly perfect lattice match for the two semiconductors. There is consensus that the room-temperature deposition of Ge leads to an abrupt heterostructure with an overlayer which is amorphous. If the substrate temperature is increased to $\sim$320 °C, however, the Ge overlayer growth is epitaxial. If the growth temperature is $\sim$520 °C, then an interdiffused, graded interface is formed. Several groups have shown that these morphological changes are accompanied by a monotonic decrease in the valence-band discontinuity, clearly indicating a dependence of the electrical properties on the structure of the interface.[5,15,16] Our studies of Ge/GaAs also show that an abrupt interface forms at room temperature but core-level analysis provides additional insight into the details of the development of chemical environments unique to the boundary layer.

In Fig. 1 we show representative Ga 3*d* and As 3*d* core-level EDC's for Ge/GaAs(110) grown at room temperature. These spectra are normalized to constant height and are offset in energy to align the position of the substrate components, thereby correcting for band bending changes. The results of line-shape decompositions are given by dashed lines. For the clean surface, the fittings reveal a surface-related Ga 3*d* doublet at 0.28 ± 0.02 eV higher binding energy than the substrate and an As 3*d* doublet at 0.39 ± 0.02 eV lower binding energy.[17,18] The bulk components are labeled 1 and the surface components are labeled 2 in Fig. 1. At these photon energies, which generate Ga and As 3*d* photoelectrons having the same kinetic energies and mean free paths, the surface contribution is 30% of the total Ga signal ($h\nu=65$ eV) and 40% of the total As signal ($h\nu=90$ eV). From this, we calculate an experimental escape depth of 4.7 Å. The fact that the surface contribution is larger for As than for

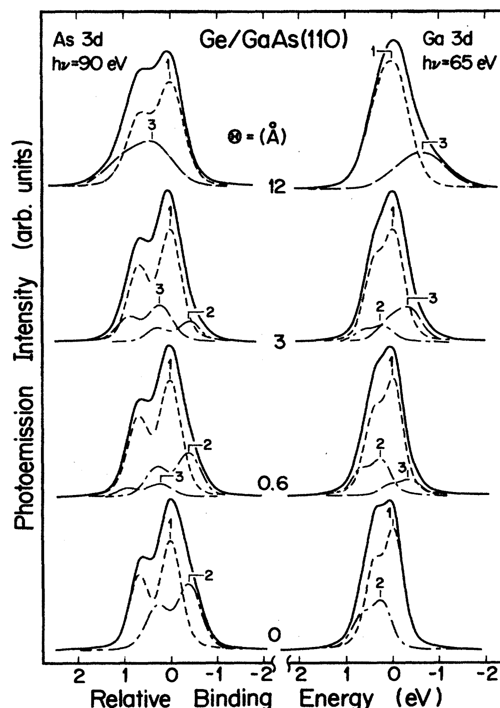

FIG. 1. Representative As 3*d* and Ga 3*d* core-level EDC's and their line-shape decompositions for amorphous Ge/*n*-type GaAs(110). The EDC's are background subtracted, normalized to the same height, and aligned to account for band bending. Components 1 and 2 correspond to emission from atoms of the substrate and surface regions. Component 3 is induced by Ge deposition and represents interface bonding.

Ga reflects the relaxation in the surface layer with As being displaced outward and Ga inward.[19] This cooperative, long-range phenomenon involves a calculated 0.35 eV per Ga-As pair.[20]

The deposition of small amounts of Ge leads to the loss of the surface components at a rate which is quite low. In contrast, when reactive metals are deposited onto these GaAs(110) surfaces, there is rapid loss of this reconstruction as surface disruption occurs. Area analysis indicates that the deposition of 1 Å of Ge reduces the As surface component from 40% to 25% of the total emission at that coverage and the Ga surface component from 30% to 20% (these relative reductions are the same to within our level of uncertainty). With Ge depositions, the substrate core level features exhibit obviously different line shapes than those for the clean cleave and attempts to fit them with only two doublets do not lead to satisfactory results. After the deposition of 3 Å of Ge, a shoulder appears on the low binding energy side of the substrate Ga $3d$ emission and there is an apparent change in the branching ratio for the As $3d$ core level. These changes clearly indicate the existence of Ge-induced interface components, labeled 3 in Fig. 1. The interface components grow as the surface components disappear but their total emission is always less than that of the substrate. At $\Theta = 12$ Å, they account for $\sim 37\%$ of the total core-level intensity (at that coverage).

To produce the fits shown in Fig. 1, it was necessary to allow the Gaussian full width at half maximum (FWHM) to increase with Ge deposition (the FWHM for As for the clean surface was 413 meV compared to 450 meV for 3 Å deposition and 580 meV for 12 Å). We attribute this broadening to disorder at the interface associated with nonepitaxial growth of Ge. In particular, the long-range surface relaxation for GaAs(110) is relatively stable and not readily disrupted by Ge adatoms. Room-temperature overlayer growth allows Ge bonding with the substrate (and therefore the appearance of the interface components) but does not induce substrate disruption or long-range cooperative relaxation. The Ge layer which forms then presents a wide range of local bonding configurations, including regions which are locally ordered and regions where bond formation is frustrated by geometric constraints. Moreover, this network is likely to evolve with deposition in the low-coverage region because of the changes in local energetics and bonding.

Quantitative analysis of the relative intensities of the surface, bulk, and interface components for Ga and As follows directly from the line-shape decompositions represented in Fig. 1. In Fig. 2, we show the resulting attenuation curves, defined as $\ln[I_i(\Theta)/I(0)]$ where $I_i(\Theta)$ is the integrated core-level intensity for component i after the deposition of Θ Å of Ge and $I(0)$ is that for the clean surface. The total attenuation curves (the sum of all components) for Ga and As are almost identical and their straight-line behavior on this semilogarithmic plot indicates average layer-by-layer growth ($1/e$ decay length of 3.9 Å, in good agreement with the experimental photoelectron mean free path for photoelectrons having ~ 42 eV kinetic energy). The correlation between the total, the substrate, and the interface component emission intensities indicates that approximately 1 ML of the substrate is altered by Ge deposition. The linear decay (on a semilogarithmic plot) of the substrate and the interface component after 10 Å indicates that substrate disruption is minimal and Ga or As presence in the Ge overlayer is very small. Additional support for uniform growth can be obtained by plotting the Ge $3d$ core-level intensity in the form $\ln[1 - I(\Theta)/I(\infty)]$. This produces a straight line on a semilogarithmic scale with slope equal to the mean free path of Ge $3d$ photoelectrons in amorphous Ge (4.1 Å measured at $h\nu = 70$ eV). Together, these results indicate that the overlayer grows in an average planar fashion with minimal tendency for Ge clustering or substrate disruption.

Figure 2 also shows the normalized intensities for each Ga and As component as a function of coverage. As can be seen, the substrate components attenuate at rates that are equal to those for the total emission while the surface components decay more rapidly (but slower than for deposition of such adatoms as Ti or even Au, as noted above). Indeed, the decay of the surface component is correlated to the appearance of component 3, the inter-

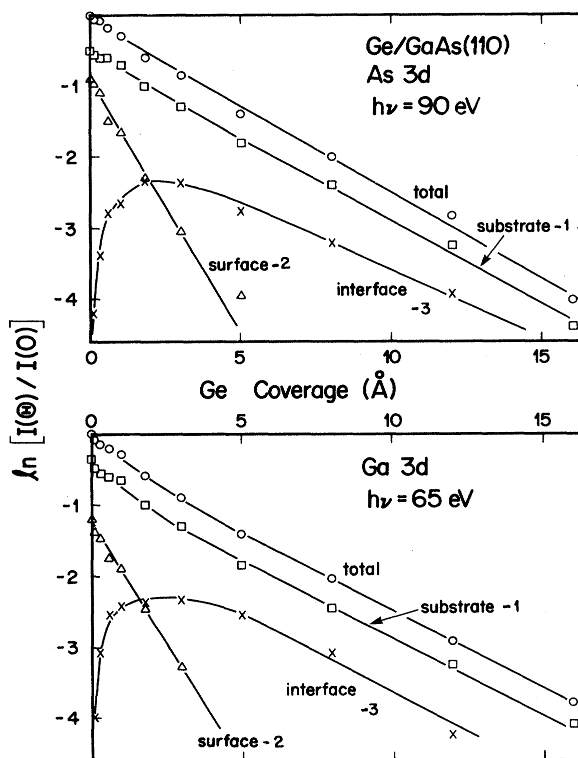

FIG. 2. As $3d$ and Ga $3d$ component-specific attenuation curves where the intensity of each component at each coverage is normalized to that for the clean surface. While no Ge-induced disruption was observed, as reflected by the exponential decay of the substrate component, the surface component decayed very rapidly because of changes in surface bonding. These same changes were reflected in the appearance of the interface component. At higher coverage, the interface component decays at a rate equal to that of the substrate.

face component, a fact we associate with gradual changes in the uppermost layer(s) of the GaAs(110) surface during Ge deposition. From our results, it can be inferred that the deposition of several monolayers of Ge is needed to fully convert the vacuum/GaAs(110) interface into the amorphous-Ge/GaAs(110) interface. The persistence of the surface component can be understood as a consequence of disordered overlayer growth, combined with the lack of chemical disruption at the interface. It has not been observed for metal/GaAs systems because of the tendency of most of these systems to induce surface disruption, to a greater or lesser extent.

In order to correlate changes in surface structure with changes in the surface electronic energy levels, we show in the upper panel of Fig. 3 the varying position of the Fermi level E_F relative to the GaAs conduction-band minimum (CBM) as a function Ge deposition. These dependences were determined from the Ga 3*d* and As 3*d* core-level EDC's measured with two different photon energies. At low coverage, E_F moves rapidly into the band gap, showing a minimum energy position at 800±30 meV below the CBM at ~3 Å, and then moves slowly back toward the conduction band to reach a value of 620 meV from the CBM at $\Theta=16$ Å. This intriguing behavior, which is much more pronounced for Ge/InP(110) (lower panel of Fig. 3), shows that the Fermi-level position must be correlated with the evolving overlayer rather than with a single type of substrate defect. Such changes must be taken into account when determining heterojunction band discontinuities.

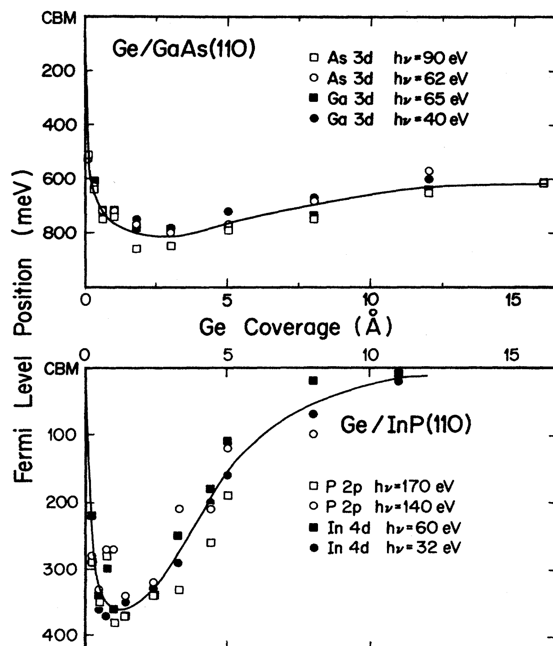

FIG. 3. Fermi-level position for amorphous Ge/*n*-type GaAs(110) and amorphous Ge/*n*-type InP(110) referenced to the conduction-band minimum (CBM) of the substrates as a function of Ge coverage. The rapid movement of E_F into the gap at low coverage is balanced by a slower return toward the CBM at higher coverage.

In order to further examine the kinetic constraints of Ge/GaAs interface formation, we undertook a low-temperature study of Ge overlayer formation on GaAs(110) at ~60 K. These results are very similar to those at room temperature but with faster attenuation of the substrate features (1/*e* decay length of 3.4 Å). The final position of the Fermi level was the same as that observed at room temperature (620 meV from CBM) but the overshoot at low coverage was almost negligible. This suggests that two competing phenomena are responsible for the Fermi-level position evolution at low coverages and that one of them is inhibited at low temperatures.

In the top of Fig. 4 we summarize our observations of the evolving energy levels for Ge/*n*-type GaAs(110), using the results of Fig. 3 to distinguish band bending changes and analysis of the valence bands to follow changes in the valence-band discontinuity. Significantly, the amorphous Ge-GaAs(110) valence-band discontinuity

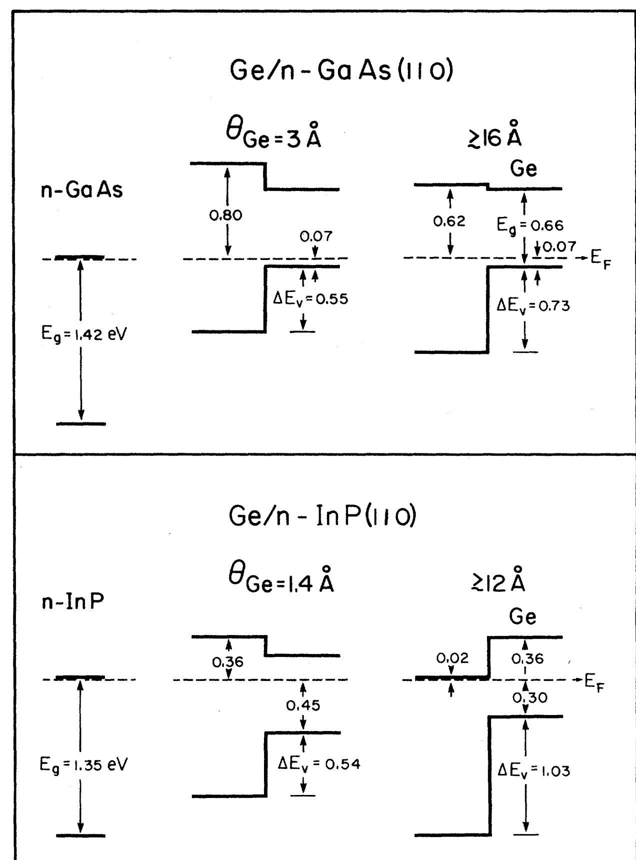

FIG. 4. Schematic energy-band diagram showing the band discontinuity and Fermi-level position at the interface for amorphous Ge/*n*-type GaAs(110) and amorphous Ge/*n*-type InP(110). The level diagrams at the right correspond to the fully established configuration. Those in the middle refer to the cases where the Fermi level is farthest from the CBM, namely the low-coverage regime before the overlayer is fully developed.

changes continuously with coverage from 550 meV at $\Theta=3$ Å to 730±80 meV at $\Theta=16$ Å. (The error estimate represents the simple sum of our uncertainties in determining core-level shifts, ±30 meV, and valence-band maxima differences, ±50 meV. Figure 3 shows the scatter in the former.) Despite this continuous change in band discontinuity, we observe *no* energy changes relative to E_F for either the top of the Ge valence band or the Ge 3*d* core-level position for coverages greater than ~3 Å. Instead, the changes in band offset reflect the movement of substrate GaAs energy levels relative to E_F, as demonstrated by the band bending results of Fig. 3. The results of Fig. 4 indicate that the amorphous Ge overlayer is *p*-type and that the conduction-band offset is very small. (Reference 21 showed that vacuum-deposited Ge overlayers on several substrates are effectively *p* type.)

Ge/*n*-type InP(110)

Studies of Ge/InP(110) and Ge/InSb(110) were undertaken so that the correlations of structure and properties discussed above for Ge/GaAs(110) could be extended to III-V systems with different tendencies for epitaxy and reaction. These systems have not been studied as extensively as Ge/GaAs(110) and they do not present particularly good lattice matches (~4% for Ge/InP and 14% for Ge/InSb). For them, the band offsets might be expected to depend on how the mismatch was accommodated at the interface, i.e., structural details of the interface which would not be included in theories of ideal interfaces. As we will show, these heterojunctions are not abrupt, even at room temperature, because Ge deposition induces substrate disruption and significant outdiffusion of In for Ge/InP(110) and In and Sb for Ge/InSb(110).

In Fig. 5 we show representative P 2*p* and In 4*d* core-level EDC's for the growing Ge/InP(110) heterostructure. As has been discussed in detail elsewhere,[22] the clean surface results reveal surface components shifted 0.30 eV to higher binding energy for In and 0.29 eV to lower binding energy for P. The deposition of 1 Å of Ge at room temperature leads to new components for both In and P (no. 3) and the reduction of the surface components (no. 2). Again, the rate of loss of the surface components is lower than observed for reactive metal overlayers. For this heterojunction, the Ge-induced component grows in relative intensity so that it is almost as intense as the substrate component by ~3 Å. At higher coverages, such as the 8-Å deposition shown in Fig. 5, component 3 dominates the spectrum. We associate these doublets with In and P atoms that have been released from the substrate. Comparison to the results for Ge/GaAs(110), where the Ge-induced Ga or As component never dominates the spectrum, indicates that the origin of the new component is quite different for these two interfaces.

Quantitative analysis of the In and P intensities of Fig. 5 makes it possible to construct the total and component-specific attenuation curves of Fig. 6. Comparison to those for Ge/GaAs strengthens the case that the distribution of substrate atoms is quite different for Ge/InP and for Ge/InSb. For Ge/InP, the loss of the

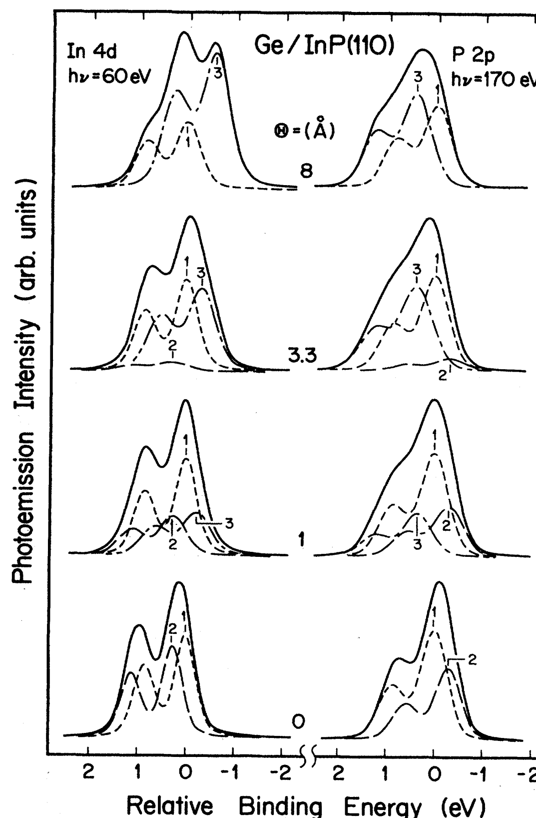

FIG. 5. Representative In 4*d* and P 2*p* core-level EDC's as a function of Ge deposition for the Ge/InP(110) interface. Components 1 and 2 correspond to bulk and surface atoms, respectively, and component 3 reflects Ge-induced disruption of the substrate. For In, component 3 is associated with atoms expelled to the surface region while the P component 3 is related to atoms in new chemical environment at the buried interface.

surface component is substantially faster (it is negligible at 3–4 Å) and the rate of growth of component 3 is faster. At higher coverage, emission from In no. 3 (expelled) exceeds the substrate component and, thereafter, it decays very slowly. Its persistence indicates that the responsible In atoms are expelled from the growing Ge overlayer and segregated to the surface and near-surface regions. In contrast, the P 2*p* attenuation curves show that P no. 3 emission exceeds the substrate emission after ~5 Å but that it decays at approximately the same rate as the substrate at higher coverage, indicating that the atoms are retained close to the interface.

The results of Fig. 6 show an interesting behavior at low coverages of 0.5–1.4 Å. In that coverage region, Ge deposition produces small changes in signal intensities for In, P, Ge, and even the surface component. At a critical coverage between 1.4 and 2.4 Å, however, the Ge signal abruptly increases and substrate intensities are attenuated. (For simplicity, we have normalized the Ge growth curve to unity at a coverage of 70 Å.) This plateau can be explained by cluster formation and growth on the surface. The observed critical coverage probably corre-

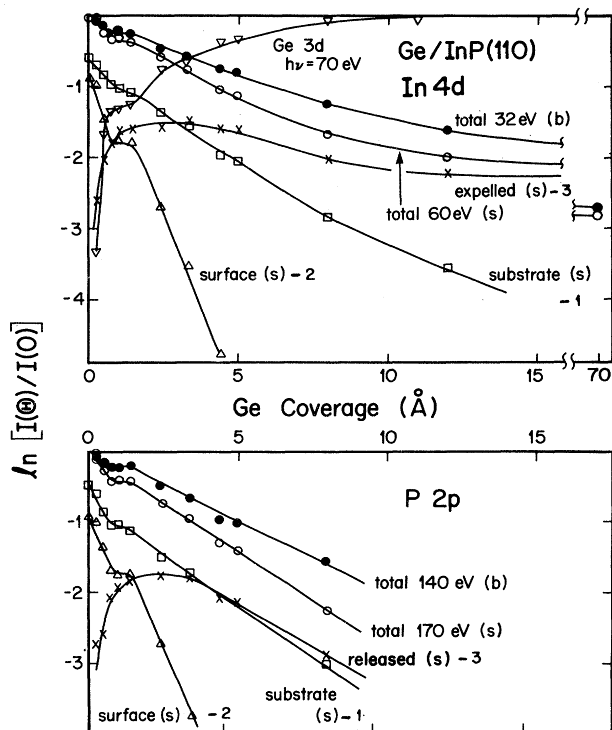

FIG. 6. Normalized core-level emission intensities for the Ge/InP(110) as a function of Ge deposition. The symbol *s* denotes surface-sensitive measurements while *b* denotes more bulk-sensitive measurements. Each of these spectra shows a plateau at 0.5–1.4 Å followed by a critical coverage at 1.4–2.5 Å associated with structural changes at the surface. In this range of coverages, the Fermi level has reached its lowest energy in the band gap. At higher coverage, the results for P indicate attenuation of all components with equal rates, revealing little redistribution of those atoms as the Ge layer thickens. For In, however, there is evidence for continued segregation and solution in the overlayer.

sponds to the misfit accommodation of these surface clusters. Although the details of the process are not known, the redistribution of atoms that occurs in this coverage range appears to be responsible for the change in direction of the Fermi-level movement and its subsequent rise toward the CBM (following paragraphs).

Additional insight into the morphology of the interface was obtained by comparing the In 4*d* binding energies for Ge/InP to those for systems where In was known to form clusters, namely In deposition onto InP(110) and onto Co interfaces.[22] Analysis shows that the energy position for In released at the Ge/InP interface differs from that for In clusters because the cluster energy is ~230 meV lower. Moreover, the In 4*d* line shapes are different for segregated In and for In clusters. In particular, the line shape of segregated In atoms (In no. 3) can be described by a symmetric Voigt function while the Doniach-Sunjic asymmetry, which is needed to describe metallic screening of the core hole, was found to be 0.16 for In clusters. These results argue against cluster formation and in favor of a more dispersed segregated In distribution on the Ge surface.

To further examine the distribution of P and In following Ge-induced disruption, we undertook a series of sputter-depth profile studies, using x-ray photoemission to monitor the intensity of the In 4*d*, P 2*p*, and Ge 3*d* photoelectrons. For these measurements, the Ar^+-ion energy was 1 keV, the photoelectron take-off angle was 60° with respect to the surface normal, the photon energy was 1486.6 eV from a monochromatized Al $K\alpha$ x-ray source, and the differentially pumped Leybold Heraeus sputter gun made it possible to keep the pressure in the measurement chamber below 2×10^{-8} Torr. Under these conditions, the effective probe depth was ~23 Å. The photoemission intensities were corrected by their cross-section ratios as measured for the clean surface, and the Ge 3*d* emission was set to unity for a thick film. Sputter-depth profiling is well known to provide a direct way of assessing relative atomic distributions.[23]

In Fig. 7 we show the results of sputter depth profiling of the 70-Å Ge/InP(110) interface. Even before sputtering, there is clear evidence for the presence of In at the surface and the amount increases steadily with sputtering time. In contrast, no P is observed until ~20 min of sputtering. The final intensity of P 2*p* is lower than that of In 4*d* because of preferential anion removal. These results complement the EDC's and attenuation curves of Figs. 5 and 6 by pointing to preferential retention of P near the buried interface and the expulsion of In into the Ge layer.

In the lower panel of Fig. 3 we show the Ge-induced movement of E_F in the band gap of *n*-InP(110). For Ge depositions below ~1.4 Å, E_F moves rapidly, reaching an extreme value of 360 meV below the CBM. This trend is reversed with additional Ge deposition, corresponding

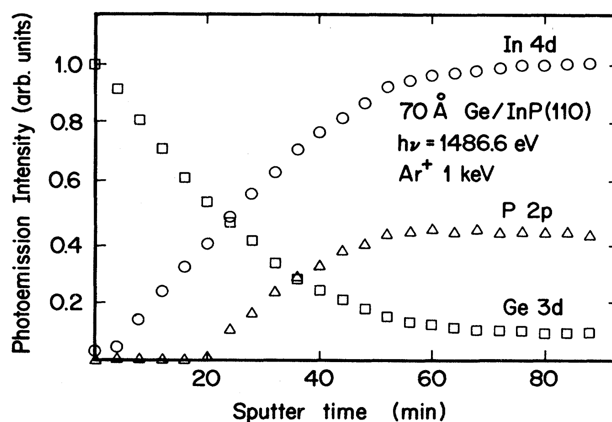

FIG. 7. Core-level intensities measured by XPS sputter depth profiling for the interface formed by the deposition of 70 Å of Ge on InP(110). Substrate species intensities are corrected by their cross-section ratio. Surface sensitivity is enhanced by the shallow angle of detection (30° from the horizon). Profiles clearly show the presence of In at the surface and in the overlayer. The final intensity for P 2*p* is lower than that for In 4*d* because of preferential sputtering of P atoms.

to the critical coverages noted above, and E_F recovers to within ~20 meV of the CBM by 12 Å deposition. This overshoot and return for InP is analogous to that shown at the top of Fig. 3 for Ge/n-type GaAs but the high-coverage correction is much larger for InP.

This interesting reversal in the movement of the Fermi level as a function of adatom deposition has also been observed by Mahowald *et al.*[24] for Ge/InP(110). They attributed it to heavy doping of the Ge overlayer by the shallow donor levels of P. The present results correlate the Fermi-level reversal with the coverage at which the In no. 3 component becomes dominant in the In 4d EDC's and In is expelled, $\Theta=2.4$ Å. The data also show that P remains trapped close to the buried InP(110) substrate. Hence, the doping of the Ge is very nonuniform across the junction. It is also likely to be nonuniform parallel to the surface because of the details of disruption and atom redistribution.

Similar Fermi-level behavior has, of course, been observed during metal-semiconductor interface formation in such diverse systems as Ti/Si(111),[25] V/Ge(111),[25] and Tm/GaAs(110).[26] From these various studies, it is clear that the final Fermi-level position is not established until the overlayer is fully developed. Although band bending at very low coverage might be described by a defect-level pinning mechanism, it is the evolution of the overlayer which appears to dictate the final behavior.

For Ge/n-type GaAs(110), we noted that the Ge valence-band maximum remained fixed after the deposition of ~3 Å and that changes in the band discontinuity reflected the movement of the GaAs VBM away from E_F. For Ge/n-type InP(110), the Ge valence bands evolve much more slowly, reflecting the incorporation and redistribution of released P and In atoms in the Ge matrix. By $\Theta > 12$ Å, E_F stabilized 0.30 eV above the VBM of Ge. By this coverage, the amorphous Ge/n-type InP(110) valence-band discontinuity had converged to 1.03 ± 0.08 eV. The evolution of the band extremes for Ge and InP are shown in Fig. 4.

Ge/n-type InSb(110)

In Fig. 8 we show the In 4d core-level emission for the cleaved InSb(110) surface, together with its decomposition into bulk (no. 1) and surface components (no. 2). The clean surface line-shape fits were obtained by analysis of spectra taken over a range of photon energies such that the surface-to-bulk ratio changed, as discussed in detail elsewhere.[22] The surface core level is shifted to higher binding energy by 0.22 ± 0.02 eV. From its contribution to the total signal intensity, the experimental inelastic mean free paths were estimated to be ~11 and ~4 Å for $h\nu=32$ and 60 eV, respectively. The deposition of Ge induces a new component (no. 3) at ~0.16 eV lower binding energy than the substrate bulk component. As for InP, it grows gradually with Ge deposition and ultimately dominates the spectrum while exhibiting no line-shape asymmetry which would indicate the formation of metallic clusters. Parallel studies of the Sb 4d core-level emission showed almost no change and attempts to fit these spectra did not produce unique solutions.

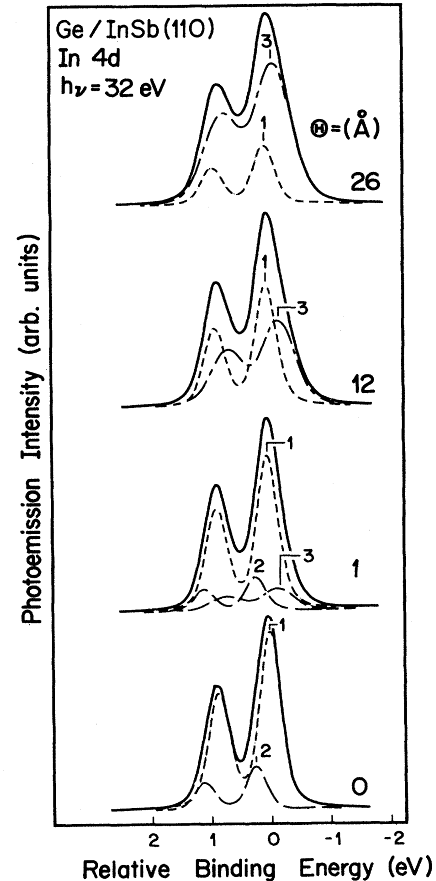

FIG. 8. Representative In 4d EDC's and line-shape analysis for the amorphous Ge/InSb(110) interface. Components 1–3 correspond to In atoms in the substrate, at the surface, and those which have been released into the overlayer.

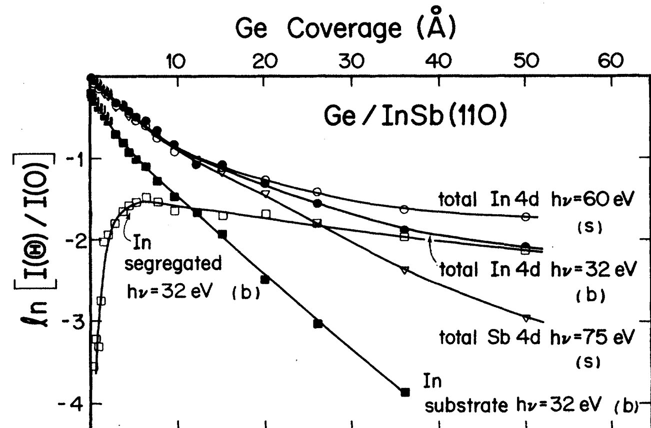

FIG. 9. In 4d and Sb 4d attenuation curves for amorphous Ge/InSb(110) showing the exponential decay of the In substrate emission after the initial disruption is complete, the growth of a component corresponding to segregated In, and the persistence of this In emission to high coverage as the atom distribution evolves. For Sb, the substrate emission attenuates at the same rate as the In substrate emission so that the high-coverage emission reflects Sb atoms released from the substrate. For simplicity, the surface component has been omitted.

In Fig. 9 we show attenuation curves defined from the total In and Sb core-level intensities taken in the surface-sensitive mode, as well as for In taken with greater bulk sensitivity at $h\nu=32$ eV. For $\Theta > 15$ Å, the In substrate intensity decreases with a $1/e$ length of ~ 10 Å, as expected for uniform overlayer growth ($h\nu=32$ eV). The faster attenuation at low coverages indicates substrate disruption and chemical conversion of the substrate component to that identified with segregation. There is then a considerable amount of dissociated In at the surface, e.g., an intensity $\sim 20\%$ of that of the clean cleaved surface even after the deposition of 50 Å of Ge ($h\nu=60$ eV).

For InSb, the band gap is only 0.17 eV and Fermi-level movements are small. Nevertheless, a behavior similar to that reported for InP was observed. The measured valence-band discontinuity was 0.12 ± 0.08 eV, in reasonable agreement with the results presented in Ref. 12.

CONCLUSIONS

Our results show that the amorphous Ge/InP(110) and Ge/InSb(110) heterostructures are far from abrupt when grown at room temperature. Even for Ge/GaAs(110), which is almost perfectly matched and composed of atoms following each other in the Periodic Table, clear changes in core-level line shapes were found that reflected bonding configurations unique to the interface. These results provide further evidence that the band lineup and the Fermi-level position do not necessarily have unique values for a given heterostructure but can depend on the details of the interface. The challenge is then to control those details and to correlate them with the electronic properties of the heterojunction.

Among many theoretically calculated values, our experimental results for Ge/GaAs(110) and Ge/InP(110) grown at 300 K are in good agreement with those recently reported by Harrison and Tersoff.[27] Their tight-binding theory predicts valence-band discontinuities of 0.66 and 1.09 eV for Ge/GaAs and Ge/InP, respectively. However, their result for Ge/InSb of 0.60 eV differs from the experimental finding.

The electron affinity rule can also lead to valence-band offsets that are in very good agreement with our experimental results. In particular, van Laar and co-workers[28] reported ionization energies of 5.56 eV for GaAs (110), 5.85 eV for InP(110), and 4.90 eV for InSb(110). Combining these with the ionization energy of 4.80 eV for Ge(111) reported by Gobelli and Allen[29] gives offsets of 0.76 eV for Ge/GaAs, 1.05 eV for Ge/InP, and 0.1 eV for Ge/InSb. Although there are different results if the data of others are used, the excellent agreement based on the electron affinity rule suggests applicability to these interfaces.[30]

Finally, we note that experimental errors can be introduced by imprecise core-level line-shape analysis and these will be reflected in the offset energies. For example, if only one Ga $3d$ doublet is considered for the Ge/GaAs(110) system, then the difference in estimating the band discontinuity can be as large as 0.12 eV. For Ge/InP(110), the error can be as large as 0.73 eV if band bending corrections are determined from the In $4d$ core-level position without considering the existence of the surface component and the interface is assumed to be abrupt.

ACKNOWLEDGMENTS

This work was supported by the Army Research Office under Grant No. DAAL-88-K-0093. One of us (C.M.A.) was supported in part by the Consejo Nacional de Investigaciones Científicas y Técnicas de la República Argentina. The synchrotron radiation photoemission experiments were conducted at the Wisconsin Synchrotron Radiation Center, which is supported by the National Science Foundation, and the support of the personnel of that laboratory is gratefully acknowledged. Correspondence with J. L. Freeouf is gratefully acknowledged. Core-level line-shape analysis was done with IBM PC-RT's made available by an IBM Materials Science and Processing Grant.

[1] H. Kroemer, Surf. Sci. **132**, 543 (1983).
[2] A. G. Milnes and D. L. Feuch, *Heterojunctions and Metal-Semiconductor Junctions* (Academic, New York, 1972); F. Capasso and G. Margaritondo, *Heterojunction Band Discontinuities: Physics and Device Applications* (North-Holland, New York, 1987).
[3] G. Margaritondo, Surf. Sci. **168**, 439 (1986).
[4] F. Capasso, Surf. Sci. **132**, 527 (1983); **142**, 513 (1984); J. Vac. Sci. Technol. B **3**, 457 (1983).
[5] R. S. Bauer and H. W. Sang, Surf. Sci. **168**, 479 (1986).
[6] J. A. Van Vechten, J. Vac. Sci. Technol. B **3**, 1240 (1985).
[7] W. R. Frensley and H. Kroemer, Phys. Rev. B **15**, 2642 (1977); O. Von Ross, Solid State Electron **23**, 1069 (1980); M. L. Cohen, Adv. Electron. Electron Phys. **51**, 1 (1980); J. Tersoff, Phys. Rev. B **30**, 4874 (1984); C. G. Van de Walle and R. M. Martin, Phys. Rev. B **35**, 8154 (1987); A. Muñoz, J. Sanchez-Dehesa, and F. Florez, Phys. Rev. B **35**, 6468 (1987); W. A. Harrison, J. Vac. Sci. Technol. B **3**, 1231 (1985).
[8] J. R. Waldrop, R. W. Grant, S. P. Kowalczyk, and E. A. Kraut, J. Vac. Sci. Technol. A **3**, 835 (1985).
[9] S. P. Kowalczyk, E. A. Kraut, J. R. Waldrop, and R. W. Grant, J. Vac. Sci. Technol. **21**, 482 (1982).
[10] M. P. Seah and W. A. Dench, Surf. Interface Anal. **1**, 2 (1979).
[11] J. J. Joyce, M Del Guidice, and J. H. Weaver, J. Electron Spectrosc. Relat. Phenom. **49**, 31 (1989).
[12] A. D. Katnani and G. Margaritondo, Phys. Rev. B **28**, 1944 (1983).
[13] R. S. List and W. E. Spicer, J. Vac. Sci. Technol B **6**, 1228 (1988).
[14] A. D. Katnani, P. Chiaradia, H. W. Sang, Jr., P. Zurcher, and R. S. Bauer, Phys. Rev. B **31**, 2146 (1985).
[15] W. Mönch, R. S. Bauer, H. Gant, and R. Murschall, J. Vac. Sci. Technol. **21**, 498 (1982).
[16] J. R. Waldrop, E. A. Kraut, S. P. Kowalczyk, and R. W. Grant, Surf. Sci. **132**, 513 (1983).
[17] T. Miller and T. C. Chiang, Phys. Rev. B **29**, 7034 (1984).

[18]D. E. Eastman, T. C. Chiang, P. Heimann, and F. J. Himpsel, Phys. Rev. Lett. **45**, 6569 (1980).
[19]A. Kahn, Surf. Sci. Rep. **132**, 193 (1983).
[20]G.-X. Qian, R. M. Martin, and D. J. Chadi, Phys. Rev. B **37**, 1303 (1988).
[21]J. E. Davey, Appl. Phys. Lett. **8**, 164 (1966).
[22]C. M. Aldao, I. M. Vitomirov, F. Xu, and J. H. Weaver, Phys. Rev. B **37**, 6019 (1988).
[23]F. Xu, C. M. Aldao, I. M. Vitomirov, Z. Lin, and J. H. Weaver, Phys. Rev. B **36**, 3495 (1987); D. M. Hill, F. Xu, Z. Lin, and J. H. Weaver, *ibid.* **38**, 1893 (1988).
[24]P. H. Mahowald, T. Kendelewicz, K. A. Bertness. C. E. McCants, M. D. Williams, and W. E. Spicer, J. Vac. Sci. Technol. B **5**, 1258 (1987); P. H. Mahowald and W. E. Spicer, *ibid.* A **6**, 1539 (1988).
[25]M. del Giudice, J. J. Joyce, M. W. Ruckman, and J. H. Weaver, Phys. Rev. B **35**, 6213 (1987) for Ti/Si(111); **32**, 5149 (1985) for V/Ge(111).
[26]M. Prietsch, M. Domke, C. Laubschat, and G. Kaindl, Phys. Rev. Lett. **60**, 436 (1988).
[27]W. A. Harrison and J. Tersoff, J. Vac. Sci. Technol. B **4**, 1068 (1986).
[28]J. van Laar, A. Huijser, and T. L. van Rooy, J. Vac. Sci. Technol. **14**, 894 (1977).
[29]G. W. Gobelli and F. G. Allen, Phys. Rev. **137**, A245 (1965).
[30]J. L. Freeouf and J. M. Woodall, Surf. Sci. **168**, 518 (1985).